International Journal of Applied Earth Observations and Geoinformation 108 (2022) 102730

Contents lists available at ScienceDirect

International Journal of Applied Earth Observations and Geoinformation

journal homepage: www.elsevier.com/locate/jag

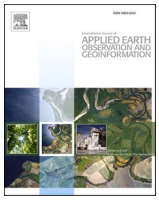

Spatio-temporal prediction of soil moisture using soil maps, topographic indices and SMAP retrievals

Marian Schönauer [a,*], Robert Prinz [b], Kari Väätäinen [b], Rasmus Astrup [c], Dariusz Pszenny [d], Harri Lindeman [b], Dirk Jaeger [a]

[a] Department of Forest Work Science and Engineering, University of Göttingen, Göttingen, Germany
[b] Natural Resources Institute Finland (Luke), Helsinki, Finland
[c] Norwegian Institute of Bioeconomy Research (NIBIO), Ås, Norway
[d] Warsaw University of Life Sciences – SGGW, Warsaw, Poland

ARTICLE INFO

Keywords:
Soil Moisture Active Passive (SMAP)
Trafficability prediction
Machine learning
Forest operations
Precision forestry
eXtreme Gradient Boosting

ABSTRACT

Milder winters and extended wetter periods in spring and autumn limit the amount of time available for carrying out ground-based forest operations on soils with satisfactory bearing capacity. Thus, damage to soil in form of compaction and displacement is reported to be becoming more widespread. The prediction of trafficability has become one of the most central issues in planning of mechanized harvesting operations.

The work presented looks at methods to model field measured spatio-temporal variations of soil moisture content (SMC, [%vol]) – a crucial factor for soil strength and thus trafficability. We incorporated large-scaled maps of soil characteristics, high-resolution topographic information – depth-to-water (DTW) and topographic wetness index – and openly available temporal soil moisture retrievals provided by the NASA Soil Moisture Active Passive mission. Time-series measurements of SMC were captured at six study sites across Europe. These data were then used to develop linear models, a generalized additive model, and the machine learning algorithms Random Forest (RF) and eXtreme Gradient Boosting (XGB). The models were trained on a randomly selected 10% subset of the dataset.

Predictions of SMC made with RF and XGB attained the highest R^2 values of 0.49 and 0.51, respectively, calculated on the remaining 90% test set. This corresponds to a major increase in predictive performance, compared to basic DTW maps ($R^2 = 0.022$). Accordingly, the quality for predicting wet soils was increased by 49% when XGB was applied (Matthews correlation coefficient = 0.45).

We demonstrated how open access data can be used to clearly improve the prediction of SMC and enable adequate trafficability mappings with high spatial and temporal resolution. Spatio-temporal modelling could contribute to sustainable forest management.

1. Introduction

Topography-derived modelling, based on digital elevation models presents a plethora of potential applications to the forestry industry. For example, Echiverri and Ellen Macdonald (2020) detected forest specific responses between species richness and a cartographic wetness index, Oltean et al. (2016) delineated drought-prone areas through moisture modelling, while Jones and Arp (2019) demonstrated the relationship between predicted soil moisture and soil strength. Specifically, accurate information of soil strength is one of the most significant parameters in ground-based forest operations. Predictions of soil strength are subsequently sought by forest managers, motivated by practical needs to enable efficient and environmentally sound forest operations (Akumu et al., 2019).

The use of modern forest machines has facilitated major improvements in work safety and efficiency. To improve production efficiency,

Abbreviations: ACC, accuracy of predictions; DTW, depth-to-water; ESDB, European Soil Database; GAM, generalized additive model; GLM, generalized linear model; MCC, Matthews correlation coefficient; ML, machine learning; RF, random forest; SMAP, Soil Moisture Active Passive; SMC, soil moisture content; SSM_{SMAP}, surface soil moisture retrieved from SMAP; XGB, extreme gradient boosting.

* Corresponding author at: University of Göttingen, Department of Forest Work Science and Engineering, Büsgenweg 4, 37077 Göttingen, Germany.
E-mail addresses: marian.schoenauer@uni-goettingen.de (M. Schönauer), robert.prinz@luke.fi (R. Prinz), kari.vaatainen@luke.fi (K. Väätäinen), rasmus.astrup@nibio.no (R. Astrup), dariusz_pszenny@sggw.edu.pl (D. Pszenny), harri.lindeman@luke.fi (H. Lindeman), dirk.jaeger@uni-goettingen.de (D. Jaeger).

https://doi.org/10.1016/j.jag.2022.102730
Received 15 November 2021; Received in revised form 5 February 2022; Accepted 17 February 2022
Available online 23 February 2022

the weight of forest machines has steadily increased over the last decades (Nordfjell et al., 2019). To counter the increased weight, machine manufactures have improved machine designs with features such as additional axles, with improved tires and tracks that all reduce ground pressure (e.g. Bygdén et al., 2003; Ala-Ilomäki et al., 2021). Yet, forest operations are still frequently associated with severe soil impacts, particularly on sites with high soil moisture content. Since the bearing capacity of wet soils is often too low to withstand the forces exerted by forest machines, traffic can result in soil disturbance, such as displacement and compaction and the creation of deep ruts (Ampoorter et al., 2012; Poltorak et al., 2018). These physical impacts can initiate negative consequences for water and gas permeability, soil fauna and biota, tree regeneration, and plant growth in general (Crawford et al., 2021).

Knowledge of time periods with best trafficability characteristics for a specific location is an important information criterion for efficient operational planning (Vega-Nieva et al., 2009; Mattila and Tokola, 2019; Picchio et al., 2020). Using detailed spatio-temporal information about soil moisture and soil trafficability allows for better planning of machine and work resources, to enable environmentally sound forest operations with less impact on the site. In return, this would improve machine productivity with less delays and well-informed production estimates along the supply chain for improved scheduling of subsequent logistical processes.

Topographic modelling of wet areas has been suggested as a potential solution to predict trafficability on forest sites. The depth-to-water (DTW) concept (Murphy et al., 2009) and the topographic wetness index (TWI, Sørensen et al., 2006) consider upstream contributing areas in order to calculate indices which allow for soil moisture estimates. Whereas TWI reveals an unique map for all conditions, DTW can be used to create different map-scenarios, aiming towards a representation of overall moisture conditions on sites. However, the ability of DTW map-scenarios to represent moisture conditions was not confirmed by Schönauer et al. (2021).

Literature highlights that temporal variations of soil moisture can be derived from a wide variety of approaches and data sources (Li et al., 2021). Launiainen et al. (2019) described a method, where the influence of topography, soil, and vegetation was considered to model water discharge of forest stands. Daily grids of soil moisture are provided for all of Germany (Samaniego et al., 2010), with the focus of drought monitoring for agricultural purposes. The Soil Moisture Active Passive mission (SMAP, Reichle et al., 2020a), run by NASA, uses radar and radiometers to globally map soil moisture, and makes the resultant three-hourly retrievals, with a spatial resolution of 9 by 9 km, openly accessible. However, the coarse resolution of such data does not allow for a direct implementation in forest management. So far, neither remotely-sensed nor hydrologically modelled information of soil moisture has been merged with high-resolution topographic indices for predicting soil moisture on forest sites.

Machine learning (ML) algorithms have been repeatedly used for mapping soil properties (e.g. Keskin et al., 2019 and Baltensweiler et al., 2021), and soil moisture (Ågren et al., 2021). Yet, ML approaches were commonly trained on a relatively large portion of data, and validated on a relatively small testing set. Challenges related to the successful implementation of ML for enhanced forest management lie in the limited data availability. Extensive efforts are needed for in-field measurements, which in-turn do not allow for predictive systems with high input data demands.

In this work we investigated the possibility of creating a model which incorporates high-resolution topographic indices, openly available soil parameters, and remotely sensed soil moisture retrievals in order to predict spatio-temporal variability of in-field measured soil moisture. In particular, we wanted to assess

- the possibility to achieve spatio-temporal modelling of soil moisture by merging spatial data with daily updated remote sensing products,
- the performance of selected ML algorithms, and
- the performance and adaptability (generalizability) of models, which were trained on only a few in-field measured observations, but were used to predict temporally varying soil moisture over large areas.

2. Material and methods

Soil moisture was measured in a time-series fashion on six different forest sites, merged with other data sources, and modelled using four statistical methods. The models were tuned by a cross-validation on an 80% partition of the data. Then, generalizability of the models was assessed by restricting the training to a 10% set, and validating the models on the remaining 90% test set.

2.1. In-field measured soil moisture content (SMC)

The response variable to be modelled, **SMC** [%vol], was measured with a capacitive soil moisture meter (HH-2 moisture meter, Delta-T Devices Ltd, England), on forest sites in Finland, Germany and Poland, along 23 measuring transects, with 21 measuring points per transect (see Schönauer et al. (2021) for site characteristics and the common measurement protocol). It was observed that the moisture measurements tended to overestimate **SMC** of relatively wet soils. Therefore, values above water saturation were cut off, and the texture-specific water saturation was assigned (see Schönauer et al. (2021) for details about soil sampling and definition of saturation). Measurements were repeated monthly, executing 6 field campaigns in Finland, 11 in Germany and 10 in Poland, between September 2019 and November 2020, resulting in 2,954 observations measured on 483 positions.

Since the susceptibility towards soil displacement increases considerably above a certain threshold of moisture (McNabb et al., 2001; Poltorak et al., 2018), values of **SMC** were also transformed into a binary variable, where texture-specific field capacity was considered to classify **wet** and **non-wet** values. The field capacity was defined at 1.9 pF matrix potential, resulting in **SMC**-thresholds of 35 %vol for data measured on Finnish study sites, 42 %vol on German sites and 19 %vol on Polish sites.

2.2. Spatial and temporal predictor variables

2.2.1. European Soil Database

The European Commission - Joint Research Centre (2004) provides a harmonized soil database for Europe (ESDB) at a scale of 1:1,000,000. Herein, maps of the main soil classification, following the World Reference Base (IUSS Working Group WRB, 2015), and several additional variables (see Supplementary Information S1, European Commission and the European Soil Bureau Network, 2004) were extracted at each measuring point and added as attributes.

2.2.2. Topographic indices

Two topographic indices, depth-to-water (DTW) and topographic wetness index (TWI), were calculated for the study sites in each participating country, based on digital elevation models with high spatial resolution, as available from the National Land Survey of Finland (2 by 2 m), Bezirksregierung Köln (2020), Germany, 1 by 1 m) and the Head Office of Geodesy and Cartography (Poland, 1 by 1 m).

A DTW map was calculated, following the procedure described by Schönauer and Maack (2021). A flow initiation area of 4.00 ha was used. Values of this map were extracted at the measuring positions and saved as new variable $\mathbf{DTW_4}$ [m].

We also calculated a topographic wetness index as defined by Sørensen et al. (2006), and extracted values at each measuring position (**TWI**, dimensionless). Therefore, digital elevation models were resampled to obtain a lower spatial resolution of 5 by 5 m to achieve robust values (Southee et al., 2012). Afterwards, the function 'r.watershed' of the free toolbox GRASS GIS (Awaida and Westervelt, 2020) was run, creating the TWI map as an output.

2.2.3. Soil Moisture Active Passive mission (SMAP)

SMAP (Reichle et al., 2020a), provides soil moisture data across the globe. SMAP was launched in January 2015. Ever since, it has generated global information about surface and subsurface soil moisture, provided at a spatial resolution of 9 by 9 km. The captured brightness, and backscatter cross-section of the earths' surface is used to determine soil moisture, including corrections for vegetation and surface roughness (Entekhabi et al., 2014).

Global grids of surface soil moisture (SMAP L4, Version 5, format: HDF5) were downloaded for each measuring day in the study period. The grids were transformed into a raster stack (see Schönauer (2022) for details), containing one layer for each measuring day. Subsequently, the raster stack was used to extract values of surface soil moisture at the locations of the study sites, for each measuring day. These values were assigned to the corresponding measuring campaigns and saved as a new variable **SSM_{SMAP}** [%vol]. By this we incorporated a temporal component, which allowed for the spatio-temporal modelling.

Soil constants provided by the SMAP mission allow for a further interpretation of geophysical fields. Several numerical and categorical parameters, as available from SMAP "land model constants" were included (see Supplementary Information S2, Reichle et al., 2020b) as predictor variables for the proposed modelling approach.

2.3. Data analyses

Data were merged and analysed using the free software language R (R Core Team, 2020), interfaced with Rstudio (version 1.4.1103, RStudio, PBC, Boston, MA). Pre-processing of the predictor variables was performed (Fig. 1): the strongly skewed predictor **DTW_4** was transformed by natural logarithm, after adding a value of 0.01, since zero-values were present. Subsequently, a linear min–max-normalization (between 0 and 1) of all numerical predictors was performed (R library: "caret", Kuhn, 2020). The high amount of $>$ 100 predictor variables was checked for identifying characteristics (e.g. sample numbers in ESDB), co-variation, redundancy, and the number of factor levels being greater than one. The data used for modelling was thereby reduced to 54 predictor variables, which consisted of **SSM_{SMAP}, DTW_4, TWI**, several land model constants (SMAP), and soil properties (ESDB).

2.3.1. Data partitioning

For modelling, the full dataset was portioned into training and validation data in two different ways (Fig. 1, Table 1): (1) **Part80-20**: 80% of the measuring positions were selected to define the training set, using the factor 'study site' as an attempt to balance the class distributions within the splits. The remaining 20% were kept aside as a test set. (2) **Part10-90**: To assess generalizability of models, a second and individual partition was created, consisting of observations measured on 49 out of 483 measuring positions in the training set, and the data measured on the remaining 434 positions kept aside as a testing set. We decided to randomly select measuring positions (instead of selecting from all observations) for splitting the data, in order to avoid temporal autocorrelation.

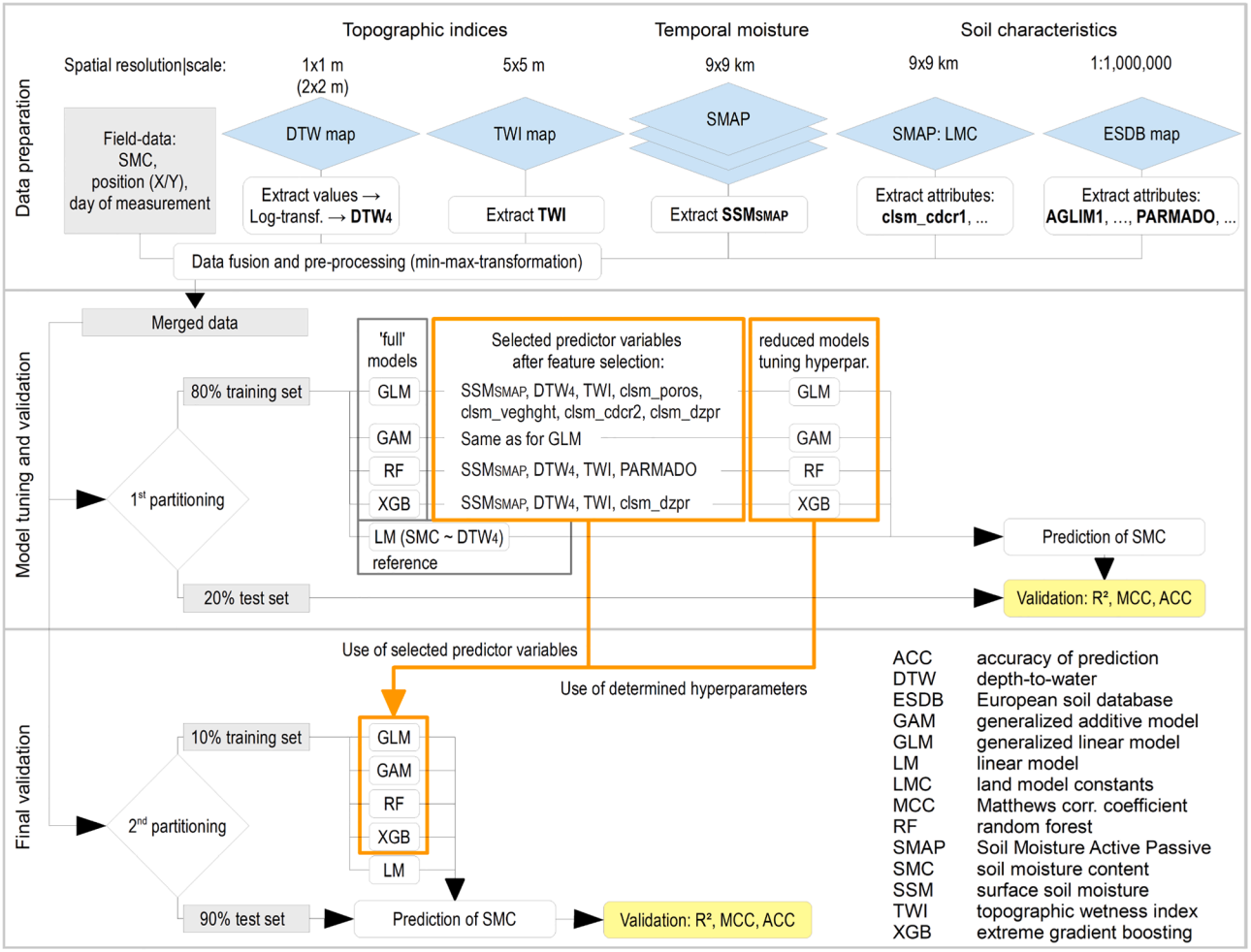

Fig. 1. Soil moisture was measured in a time-series fashion on six forest sites, merged with other data sources, and modelled using different statistical methods. A two-step modelling was conducted, in order to test generalizability of the models when predictions were made for the 90% test set.

Table 1
Amount of data used for a two-step model training and testing. Data originating from 80% or 10% of the measuring positions were used for training, whereas the remaining parts were used for model validations.

	Part80-20		Part10-90	
Site	training	testing	training	testing
Eno	396	108	36	468
Onttola	414	90	66	438
Neheim	748	176	99	825
Obereimer	536	135	64	608
POL_North	130	20	10	140
POL_South	140	60	20	180

2.3.2. Basic predictions by the topographic indices

Simple linear models were fitted to carry out regressions between **SMC** ~ **DTW$_4$** or **TWI**. This was done to calculate the coefficient of determination (R^2, equation (1)), with the inclusion of model intercepts. For predictions derived from **DTW$_4$**, Matthews (1975) correlation coefficient (MCC, equation (2)) and accuracy of predictions (ACC, equation (3)) were calculated based on the created confusion matrix (Table 2).

2.3.3. Model building and tuning

Based on existing studies that modelled spatial aspects of soil properties (Hengl et al., 2018; Ågren et al., 2021; Baltensweiler et al., 2021), four statistical modelling approaches to test in this study were identified: a generalized linear model, an additive model, and two ML algorithms.

As a first step, 'full' models, consisting of 54 predictor variables of the 80% training dataset, were reduced, until a decrease of goodness-of-fit (>1%) occurred. Then, the tuning of the reduced models was performed through a 10-fold cross-validation (R library: "caret", Kuhn, 2020), aimed at attaining the highest possible of R^2, calculated on the 10th chunks of the cross-validation.

Afterwards, the hyperparameters determined through the cross-validation (on the 80% training dataset) were used to build new models based on the 10% training set (Fig. 1). Validation of the reduced and tuned models was performed on the unseen testing datasets, either comprising of 20% or 90% of the entire dataset, respectively.

The models were used to calculate raster predictions of **SMC**, possessing a spatial resolution of the used digital elevation models (1 by 1 m for the sites in Germany and Poland, 2 by 2 m for the Finnish sites). These rasters were evaluated with respect to the reasonability of the predicted outputs.

2.3.3.1. Generalized linear model with stepwise feature selection (GLM). The goal of a GLM is to select predictors that fit the response variable well (library: "MASS", Venables and Ripley, 2002). To reduce the full model to important predictors only, Akaike's information criterion was assessed step-wise throughout the iterative variable selection procedure. The reduced model of the GLM included **SSM$_{SMAP}$**, **DTW$_4$**, **TWI**, **clsm_poros**, **clsm_veghght**, **clsm_cdcr2** and **clsm_dzpr** (Supplementary Information S2) as predictor variables. These variables were used to fit models to both training datasets, and make predictions on the corresponding testing datasets.

Table 2
Two confusion matrices were created, by comparing the occurrence of binary values of in-field measured soil moisture content **SMC** to depth-to-water values (**DTW$_4$**) or predicted values of **SMC** (after adding a constant of 5 %vol). The thresholds for the two levels of **SMC** were 35 %vol (Finland), 42 %vol (Germany) and 19 %vol (Poland).

Classification	abbr.	measured **SMC**	predicted **SMC**+ 5	**DTW$_4$** [m]
true positive	TP	**wet**	**wet**	<1
true negative	TN	**non-wet**	**non-wet**	≥1
false positive	FP	**non-wet**	**wet**	<1
false negative	FN	**wet**	**non-wet**	≥1

2.3.3.2. Generalized additive model with loess function (GAM). The GAM is a generalized linear model in which the response is fitted to predictions made with a loess smooth function (R library: "gam", Hastie, 2020). Thereby, GAM can cope with non-linear responses. For model tuning, a *span* between 5 and 50 was considered for the predictors already selected (Section 2.3.3.1).

2.3.3.3. Random forest (RF). The RF model is a tree-based learner, which randomly partitions the data into nodes, aiming to maximize the within-node homogeneity and the between-node heterogeneity (Breiman, 2001). The feature reduction was run with default settings (R library: "ranger", Wright and Ziegler, 2017, $min_{nodesize} = 5$, $m_{try}=\lfloor\sqrt{p}\rfloor$, where p is the number of predictor variables), executing a stepwise recursive elimination of the least important predictors, where five predictors were removed at once. The reduced model included **SSM$_{SMAP}$**, **DTW$_4$**, **TWI**, and **PARMADO**, and possessed the highest out-of-bag variation explained by predictions. Using these predictor variables, values of m_{try} between 1 and p, and $min_{nodesize}$ from 1 to 10 were considered for the tuning.

2.3.3.4. Extreme gradient boosting (XGB). The XGB mostly combines a number of regression trees and uses optimized distributed gradient boosting – an iterative way of putting more weight on large pseudo-residuals (R library: "xgboost", Chen et al., 2021). The full XGB model was built using a random setting of hyperparameters. Thereafter, the four most important predictors, **SSM$_{SMAP}$**, **DTW$_4$**, **TWI**, and **clsm_dzpr** were used for further tunings, following the procedure described by Ågren et al. (2021). Yet, hyperparameters were confined to conservative ranges: max_{depth} = 2, 3 and 4, eta = 0.05, 0.10 and 0.15, $rate_{drop}$ and $skip_{drop}$ = 0.25, 0.50 and 0.75, $min_{childweight}$ = 10, 20 and 30, $gamma$ = 0.8, 0.9 and 1.

2.3.4. Evaluating predictive performance

For reducing the full models to reduced/final models, and for the comparison of such to each other, goodness-of-fit was assessed. Therefore, differences between observed and predicted values, were considered to calculate R^2 (equation (1)). With observed values y_i, predicted values $\hat{y}_i$, mean values of observed values $\bar{y}$, for i observations:

$$R^2 = 1 - \frac{\sum_i (y_i - \hat{y}_i)^2}{\sum_i (y_i - \bar{y})^2} \quad (1)$$

Matthews correlation coefficient (MCC, equation (2)), and accuracy of predictions (ACC, equation (3)) were calculated on a confusion matrix between predicted and measured values (Table 2). Therefore, binaries of measured and predicted **SMC** were compared, after adding a constant of 5 %vol to model-derived predictions and applying the same texture specific thresholds.

$$MCC = \frac{TP*TN - FP*FN}{\sqrt{(TP+FP)(TP+FN)(TN+FP)(TN+FN)}} \quad (2)$$

$$ACC = \frac{TP + TN}{TP + TN + FP + FN} \quad (3)$$

3. Results

Overall moisture conditions clearly differed between the three countries with mean values of 14.0 %vol measured in Poland, 29.3 %vol measured in Finland, and 30.3 %vol measured on German study sites. Eleven consecutive measuring campaigns were conducted in Germany, resulting in mean values per measuring day and site ranging from 13.6 %vol to 44.1 %vol (Fig. 2). Lower extents of campaign-to-campaign variation could be observed on Finnish and Polish study sites, where

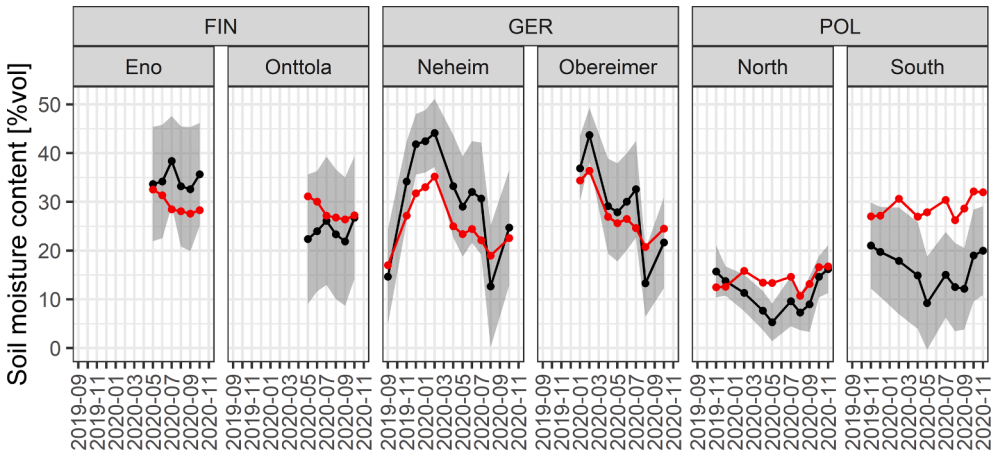

Fig. 2. Soil moisture content (**SMC**) measured on six sites in three countries (FINland, GERmany, POLand), in a time series fashion (year-month). Black dots show mean values of **SMC** for each site and day of measurement; the shading indicates the corresponding standard deviation. Red dots indicate remotely-sensed surface soil moisture ($\mathbf{SSM_{SMAP}}$), as available from the Soil Moisture Active Passive mission.

means ranged between 21.9 %vol and 38.4 %vol, and 5.3 %vol and 21.1 %vol, respectively. Overall, $\mathbf{SSM_{SMAP}}$ was in relatively close alignment with mean values of **SMC** in most of the study sites, except in 'POL_South' (Fig. 2).

3.1. Prediction of SMC

Simple linear models were used to compare **SMC** and **TWI** of the 80% training dataset, indicating a significant correlation ($p < 0.001$), but a high proportion of variation was unexplained ($R^2 = 0.049$). Another linear model was fitted to **SMC** and $\mathbf{DTW_4}$ of the 80% training dataset, revealing a significant correlation between the two variables ($p < 0.001$). The goodness-of-fit of $\mathbf{DTW_4}$ derived predictions of **SMC** was different between the measuring sites, with $R^2 = 0.16$ when only the Finnish data was considered, and $R^2 = 0.42$ for Polish data. Yet, the over-representation of German data (Table 1), where R^2 was 0.019, as well as site-specific intercepts resulted in an overall $R^2 = 0.022$ for the 80% training dataset (Fig. 3A).

Ideally, all **wet** values would coincide with $\mathbf{DTW_4} < 1$ m (Table 2). The actual occurrence of **wet** values was correctly predicted by $\mathbf{DTW_4}$ for 38% of observations (=TP/(TP + FN), Table 3), participating to a total MCC = 0.30 (Fig. 4A).

Table 3
Confusion matrix of true positives (TP), true negatives (TN), false positives (FP) and false negatives (FN), representing wet (Positive) and dry (Negative) measurements predicted by depth-to-water maps (DTW), and spatio-temporal models based on several predictors: generalized linear model (GLM), generalized additive model (GAM), random forest model (RF) and extreme gradient boosting (XGB).

	Classes of confusion matrix			
Prediction	TP	TN	FP	FN
DTW	274	1713	2230	442
GLM	459	1522	421	257
GAM	462	1521	422	254
RF	494	1488	455	222
XGB	530	1446	497	186

The ability to explain the goodness-of-fit was clearly improved when applying more predictor variables to the XGB and RF modelling approaches, compared to basic $\mathbf{DTW_4}$ predictions. R^2 calculated by the cross-validation ranged between 0.43 (GLM) and 0.80 (XGB, RF)

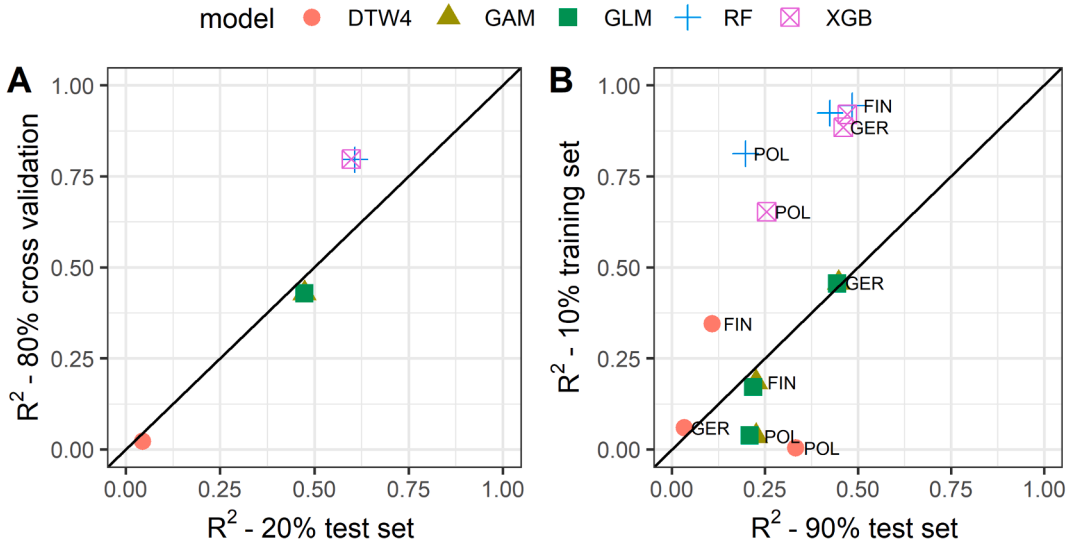

Fig. 3. Soil moisture on sites in FINland, GERmany and POLand was predicted by depth-to-water maps (DTW) and spatio-temporal models using several predictor variables: general additive model (GAM), a generalized linear model (GLM), random forest (RF) and extreme gradient boosting (XGB). R^2 (equation (1)) was calculated for the 80% training dataset (A), a 10% training dataset (B), and the remaining test sets of 20% and 90%, respectively.

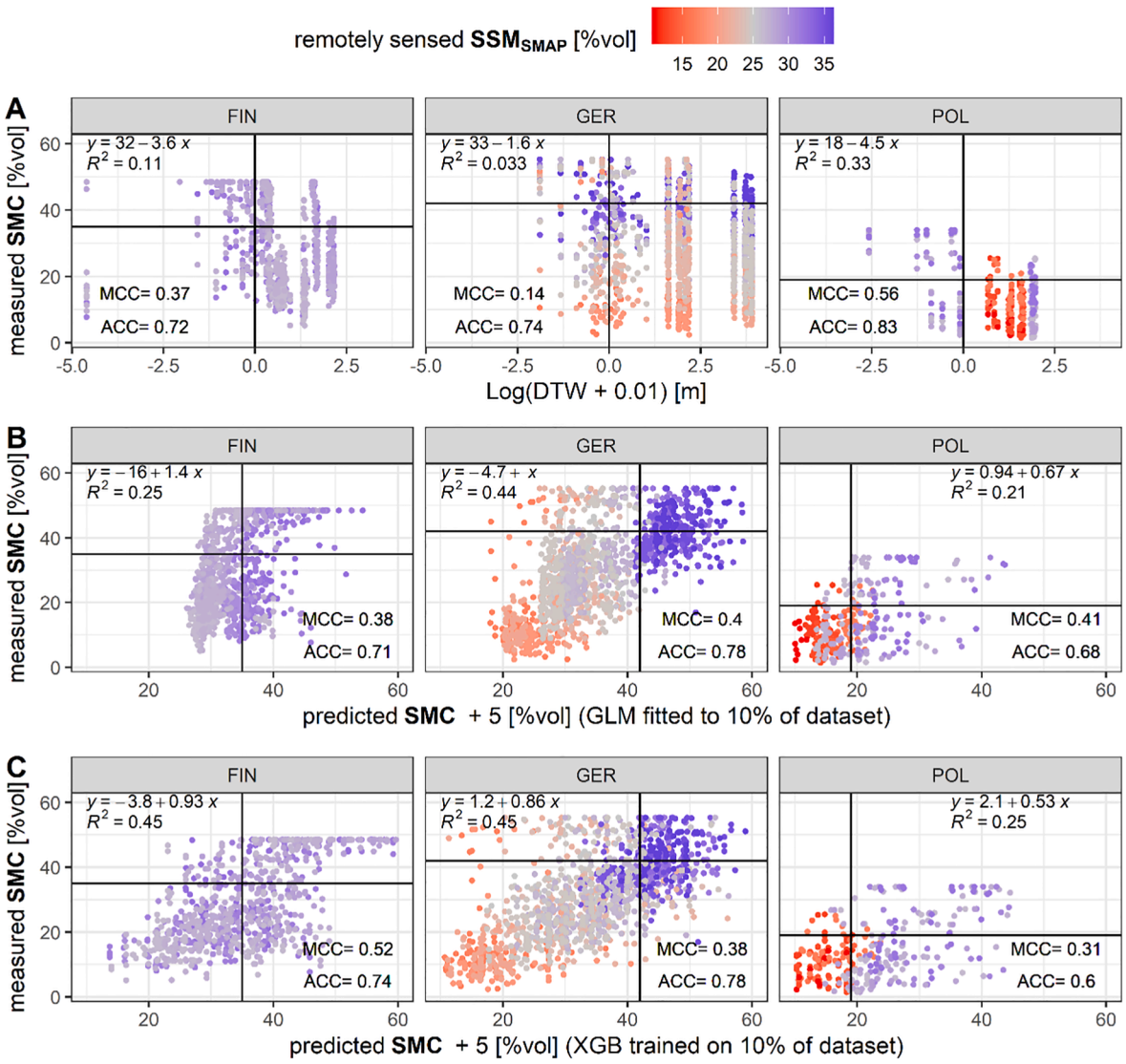

Fig. 4. Soil moisture content (SMC) was measured on forest sites in FINland, GERmany and POLand. The values were compared to depth-to-water (DTW) values (**A**). A generalized linear model (GLM, **B**) was fitted, and the machine learning algorithm extreme gradient boosting (XGB, **C**) was trained on a 10% subset of data, and used to predict SMC of the remaining 90%. Colouring indicates remotely sensed surface soil moisture (**SSM$_{SMAP}$**). With regression equations, R^2, MCC and ACC, according to equations (1), (2) and (3).

(Fig. 3A). When trained on the 80% dataset, the two ML algorithms RF and XGB revealed similar predictions of **SMC**, with a tendency towards higher R^2 for the training dataset, compared to the test dataset. When the model training was performed on the 10% set, minor differences occurred between the RF and XGB (Fig. 3B). When applied to the 90% test dataset of German sites, robust predictions were derived from the GLM (Fig. 4B) and GAM, with R^2 equal 0.44 and 0.45, respectively. However, significantly lower R^2-values were observed for the remaining observations made in Finland and Poland (Fig. 3B).

The methods RF ($n_{trees} = 500$, $m_{try} = 2$, $min_{nodesize} = 2$) and XGB ($n_{rounds} = 500$, $eta = 0.10$, $max_{depth} = 4$, $gamma = 1$, $colsample_{bytree} = 0.50$, $min_{childweight} = 5$, $rate_{drop} = 0.25$, $skip_{drop} = 0.75$, $subsample = 0.5$) were applied to the predictor variables **SSM$_{SMAP}$**, **TWI**, **DTW$_4$** and either **PARMADO** or **clsm_dzpr**, respectively. For both models, **SSM$_{SMAP}$** was the most important predictor, followed by the two topographic indices and one soil parameter. In effect, the soil parameter acted as a grouping variable, since unique values were present for each participating country (**PARMADO**, i.e. dominant parent material, derived from ESDB), or site (**clsm_dzpr**, i.e. thickness of profile soil moisture layer, derived from SMAP). Based on these predictors, RF and XGB models were trained on the 10% dataset and validated on the 90% test dataset (Fig. 4C), resulting in **SMC** predictions with an overall $R^2 = 0.49$ for both models – a significant increase compared to the simple linear model with **DTW$_4$** as independent variable ($R^2 = 0.022$). Accordingly, MCC was increased by approximately 49%, from 0.30 (**DTW$_4$**), to 0.40 (GLM) and 0.45 (XGB), calculated on the 90% test dataset.

4. Discussion

In the present study, we illustrated how spatio-temporal variation in soil moisture can be predicted and hence serve as an important tool for reduced soil impacts in forest operations. For several decades, topography derived indices have been developed, aimed at supporting low-impact forest operations through predictions of soil moisture across large landscapes, with low demands of input data. An example of such an index is DTW, introduced by Murphy et al. (2009), who intended to simulate overall moisture conditions by different map-scenarios. This concept was motivated by the urgent need of forest managers for dynamic predictions (Akumu et al., 2019), yet the ability of representing seasonal moisture conditions by DTW map-scenarios was not confirmed

in a recent study (Schönauer et al., 2021). The latter showed, that one map-scenario resulted in the highest predictive performance on a given site, across several seasonal conditions. In agreement, Ågren et al. (2014) and Mohtashami et al. (2017) showed, how differently calculated map-scenarios led to enhanced predictive performances on different sites. These predictions were driven by diverse soil-related, geomorphological and climatic influences on water accumulation on sites.

The complexity of temporal variations of moisture and spatial variations of soil characteristics, can be captured by ML approaches, which are designed to make predictions for complex phenomena with many interactions (Heung et al., 2016). Current research demonstrated and corroborated the potential of such methods for mappings of soil carbon content (e.g. Keskin et al., 2019), diverse soil characteristics (e.g. Baltensweiler et al., 2021), and for creating static moisture maps in Sweden (Lidberg et al., 2020; Ågren et al., 2021). Although temporary, dynamic maps of soil moisture have been made available by different sources (Li et al., 2021), but the low spatial resolution (e.g. 9 by 9 km, SMAP) of such would not allow for direct utilization for forest operations (Zeng et al., 2019). In this work, we demonstrated how low-resolution SMAP grids were merged with high-resolution DTW and TWI maps, resulting in a high-resolution spatio-temporal prediction of **SMC** (1 by 1 m on sites in Germany and Poland, 2 by 2 m on Finnish sites) on different sites in Europe – a system which could gain value for sustainable forest management, currently challenged by increases in climatic variability and less favourable operational conditions (Pfeifer et al., 2021). Among the investigated modelling approaches, best predictive performance was attained by two investigated machine learning algorithms. Both models can be used to create maps of **SMC** on a daily basis (Fig. 5).

Although the performance of ML models deeply relies upon the quality and quantity of input data used for training (Heung et al., 2016), a system for trafficability prediction should work on low quantities of input data – an inevitable prerequisite for achieving a practical application to enable day-to-day support for forest management over large areas. Therefore, we assessed the predictive ability of the models, when only limited input data was selected for model training. In a separate mode of modelling, the training set was confined to data captured on only 10% of the measuring points to avoid auto-correlation between repeated measurements made on identical measuring positions. The validation of the trained models on the remaining 90% test dataset revealed a reduction in predictive performance compared to the 20% test dataset. When XGB was applied, R^2-values of 0.25 and 0.45, were reached on sites in Poland, and Finland and Germany, respectively (Fig. 4). This corresponds to a more than 3-fold increase in R^2 for Finnish data, a 39%-decrease for the data measured in Poland, and an almost 14-fold increase for the data measured on German sites, compared to basic DTW predictions. The improvements of predictive performance within the data from Germany can be partly explained by the clear influence of $\mathbf{SSM_{SMAP}}$ within the ML models (Fig. 4). On German sites, the highest variations of **SMC** between the measuring days occurred – a vector that was adequately reflected by $\mathbf{SSM_{SMAP}}$ (Fig. 2).

Accordingly, MCC, an informative and truthful indicator for the assessment of classifications (Powers, 2011) was increased from 0.30 (binary values of $\mathbf{DTW_4}$) to 0.44 (XGB). It has to be noted though, that a constant of 5 %vol was added to the model-derived predictions before classifying the predicted values of SMC into **wet** and **non-wet**. We assumed, that the underrepresentation of **wet** values, which accounted for 36% of the entire dataset, led to an underestimation of such. Yet, after adjusting the predictions, 74% of **wet** values were predicted correctly (Table 3) – a considerable improvement compared to basic

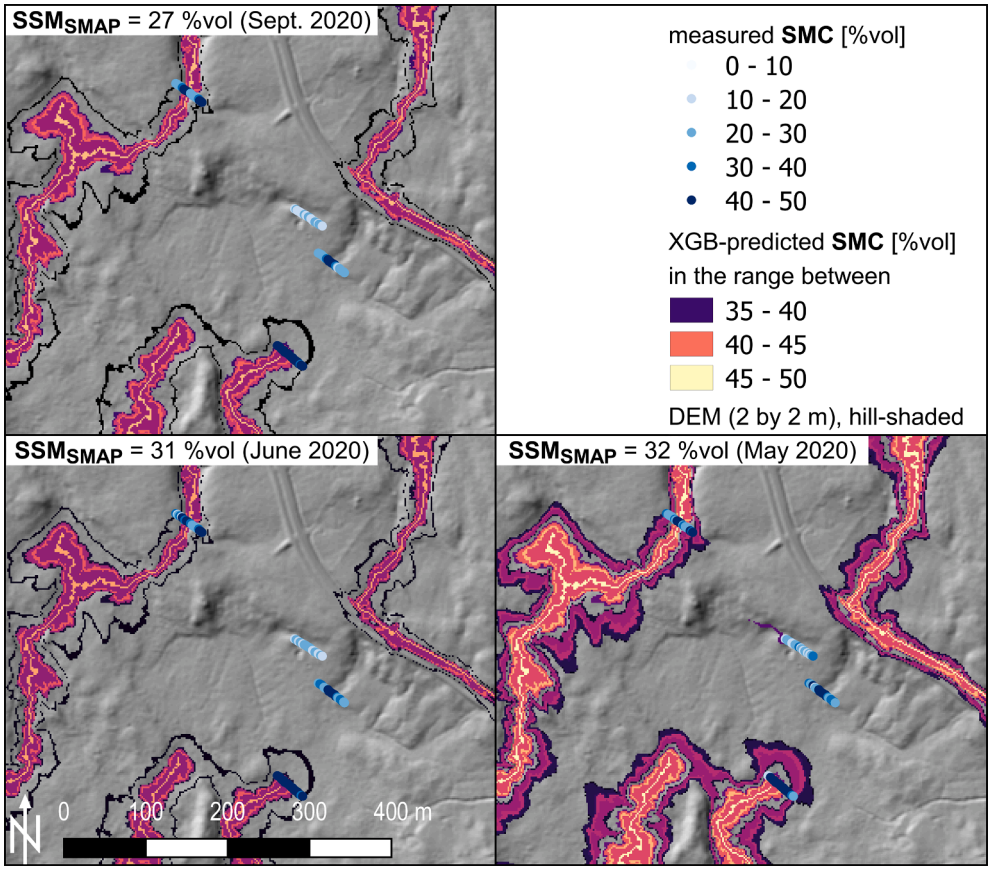

Fig. 5. A spatio-temporal modelling of soil moisture content (**SMC**) was achieved by merging spatial and temporal information, and the application of the machine learning algorithm extreme gradient boosting (XGB). Remotely sensed soil moisture ($\mathbf{SSM_{SMAP}}$), two topographic indices, based on digital elevation models (DEM), and large-scaled soil properties were used. The maps show a shaded DEM and the coloured predictions highlight the extent of wet soils (**SMC** $\geq$ 35 %vol).

DTW predictions.

Only a few predictor variables were sufficient to explain a large share of the variation in **SMC**. The initially large number of predictors was reduced to four predictors, consisting of $\mathbf{SSM_{SMAP}}$, $\mathbf{DTW_4}$, **TWI** and one soil parameter, either derived from the land model constants from SMAP (**clsm_dzpr**), or the ESDB (**PARMADO**). It was decided to include DTW maps calculated with a flow initiation area of 4.00 ha (Jones and Arp, 2019), based on three arguments: (I) DTW values from different map-scenarios were partially autocorrelated, (II) since the measuring transects were specifically located on DTW gradients (see Schönauer et al. (2021) for details), only $\mathbf{DTW_4}$ comprised of topographic gradients between the transects. When a DTW map-scenario for moister conditions was chosen, all transects would show zero-values in the centre with similar increases of DTW at the outer parts of each transect. (III) Although high explanatory power was reached when including different DTW map-scenarios, raster predictions made with such models led to unreasonable maps – an aspect which has to be accounted for when modifying the predictors (Meyer et al., 2019). When two or more DTW map-scenarios were included, chequered patterns were observed in the grid predictions made, an indicator for overfitting caused by repeated use of similar predictors and spatial autocorrelation (Nussbaum et al., 2018).

Data used for the developed modelling was openly accessible, allowing for a spatio-temporal prediction of **SMC** in all regions where high-resolution DEMs are available. The validation performed here was limited to six selected sites. However, on each site only a few repeated measurements (in this case, 10 to 99) were required to predict a total of 2,660 values of **SMC**, covering a time span of more than a year. It would be possible to consolidate moisture data of different origins, more accurate soil mappings and weather data to extend **SMC** predictions to a wide range of landscapes and seasons. Applications of created prediction maps could be manifold, including a potential utilization for modelling forest growth, agricultural purposes, drought monitoring and irrigation scheduling (Li et al., 2021). In the field of forest operations, accurate spatio-temporal predictions can support mitigating measures, and thereby enhance environmentally sound and economically efficient forestry practices as a whole.

5. Conclusion

This study showed a successful prediction of **SMC** values at six study sites in Europe. Through the utilization of machine learning, site-specific and non-linear effects on **SMC** could be captured, setting a direction for further solutions towards a large-scaled, temporal and precise support for harvesting operations. The freely available data, provided by the SMAP mission, showed to be an adequate proxy to be used for predictions of **SMC**. The variable $\mathbf{SSM_{SMAP}}$ strongly contributed to model **SMC** with the XGB and RF algorithms, along with the topography-based $\mathbf{DTW_4}$ and **TWI** and the one soil parameter. Applying the XGB resulted in MCC of 0.45, with 74% of **wet** values predicted correctly, and R^2 of 0.51 – a significant improvement compared to basic $\mathbf{DTW_4}$ derived predictions, where MCC was 0.30 (38% of **wet** values predicted correctly), and R^2 was 0.022. A 10% subset of the entire data was sufficient to predict the remaining 90%, corresponding to 10 to 99 in-field measurements necessary per site. A low demand of input data might be a crucial prerequisite to achieve a modelling approach which can be applied for day-to-day forest management. We are confident though, that increasing possibilities in modelling spatio-temporal dynamics of soil moisture, innovative and interactive sensor networks and more than anything, increasing amounts of field data, will enable further developments towards accurate predictive systems which support year-round timber mobilization with lower environmental impacts.

CRediT authorship contribution statement

Marian Schönauer: Conceptualization, Methodology, Formal analysis, Visualization, Investigation, Resources, Writing – original draft, Writing – review & editing. **Robert Prinz:** Investigation, Resources, Writing – review & editing. **Kari Väätäinen:** Investigation, Resources, Writing – review & editing. **Rasmus Astrup:** Writing – review & editing, Project administration, Funding acquisition. **Dariusz Pszenny:** Investigation, Resources. **Harri Lindeman:** Investigation, Resources. **Dirk Jaeger:** Writing – review & editing, Supervision, Project administration, Funding acquisition.

Declaration of Competing Interest

The authors declare that they have no known competing financial interests or personal relationships that could have appeared to influence the work reported in this paper.

Acknowledgements

We acknowledge the valuable suggestions of the two anonymous reviewers, who contributed to the improvement of the paper. We acknowledge the collaboration with Prof. Paul Arp and his team (Faculty of Forestry and Environmental Management, University of New Brunswick), who conceived, developed and tested the depth-to-water concept.

Funding

This work was supported by the Bio Based Industries Joint Undertaking under the European Union's Horizon 2020 research and innovation program, TECH4EFFECT Knowledge and Technologies for Effective Wood Procurement—project, [grant number 720757]; by the cooperation project "BefahrGut" funded by the State of North Rhine-Westphalia, Germany, through its Forest Education Centre FBZ/State Enterprise Forestry and Timber NRW, Arnsberg/Germany; and by the Eva Mayr-Stihl Stiftung.

Data statement

Data was made available at: https://doi.org/10.5281/zenodo.5659098.

Appendix A. Supplementary material

Supplementary data to this article can be found online at https://doi.org/10.1016/j.jag.2022.102730.

References

Ågren, A.M., Larson, J., Paul, S.S., Laudon, H., Lidberg, W., 2021. Use of multiple LIDAR-derived digital terrain indices and machine learning for high-resolution national-scale soil moisture mapping of the Swedish forest landscape. Geoderma 404, 115280. https://doi.org/10.1016/j.geoderma.2021.115280.

Ågren, A., Lidberg, W., Strömgren, M., Ogilvie, J., Arp, P., 2014. Evaluating digital terrain indices for soil wetness mapping – a Swedish case study. Hydrol. Earth Syst. Sci. 18, 3623–3634. https://doi.org/10.5194/hess-18-3623-2014.

Akumu, C.E., Baldwin, K., Dennis, S., 2019. GIS-based modeling of forest soil moisture regime classes: using Rinker Lake in northwestern Ontario, Canada as a case study. Geoderma 351, 25–35. https://doi.org/10.1016/j.geoderma.2019.05.014.

Ala-Ilomäki, J., Lindeman, H., Mola-Yudego, B., Prinz, R., Väätäinen, K., Talbot, B., Routa, J., 2021. The effect of bogie track and forwarder design on rut formation in a peatland. Int. J. Forest Eng. 32 (sup1), 12–19. https://doi.org/10.1080/14942119.2021.1935167.

Ampoorter, E., de Schrijver, A.n., van Nevel, L., Hermy, M., Verheyen, K., 2012. Impact of mechanized harvesting on compaction of sandy and clayey forest soils: results of a meta-analysis. Ann. Forest Sci. 69 (5), 533–542. https://doi.org/10.1007/s13595-012-0199-y.

Awaida, A., Westervelt, J., 2020. Geographic Resources Analysis Support System (GRASS GIS). USA: Geographic Resources Analysis Support System (GRASS GIS) Software. Accessed February 15, 2021, https://grass.osgeo.org.

Baltensweiler, A., Walthert, L., Hanewinkel, M., Zimmermann, S., Nussbaum, M., 2021. Machine learning based soil maps for a wide range of soil properties for the forested area of Switzerland. Geoderma Regional 27, e00437. https://doi.org/10.1016/j.geodrs.2021.e00437.

Bezirksregierung Köln (2020). *Digitales Geländemodell DGM1 [Digital elevation model]*. Accessed November 08, 2021, https://www.bezreg-koeln.nrw.de/brk_internet/geobasis/hoehenmodelle/digitale_gelaendemodelle/gelaendemodell/index.html.

Breiman, L., 2001. Random forests. Mach. Learn. 45, 5–32. https://doi.org/10.1023/A:1010933404324.

Bygdén, G., Eliasson, L., Wästerlund, I., 2003. Rut depth, soil compaction and rolling resistance when using bogie tracks. J. Terramech. 40 (3), 179–190. https://doi.org/10.1016/j.jterra.2003.12.001.

Chen, T., He, T., Benesty, M., Khotilovich, V., Tang, Y., Cho, H., et al. (2021). *xgboost: Extreme Gradient Boosting*. Accessed November 09, 2021, https://CRAN.R-project.org/package=xgboost.

Crawford, L.J., Heinse, R., Kimsey, M.J., Page-Dumroese, D.S., 2021. Soil sustainability and harvest operations. General Technical Report RMRS. https://doi.org/10.2737/RMRS-GTR-421.

Echiverri, L.F.I., Ellen Macdonald, S., 2020. A topographic moisture index explains understory vegetation response to retention harvesting. For. Ecol. Manage. 474, 118358. https://doi.org/10.1016/j.foreco.2020.118358.

Entekhabi, D., Yueh, S., and Lannoy, G. de (2014). *SMAP handbook: Soil Moisture Active Passive*. Accessed November 08, 2021, https://lirias.kuleuven.be/retrieve/526486.

European Commission - Joint Research Centre (2004). *European Soil Data Centre (ESDAC)*. Accessed November 09, 2021, https://esdac.jrc.ec.europa.eu.

European Commission and the European Soil Bureau Network (2004). *The European Soil Database distribution version V2.0: Attributes of the SGDBE version 4 beta*. Accessed November 09, 2021, https://esdac.jrc.ec.europa.eu/ESDB_Archive/ESDBv2/popup/sg_attr.htm.

Hastie, T., 2020. *gam: Generalized Additive Models*. Accessed November 09, 2021, https://CRAN.R-project.org/package=gam.

Hengl, T., Nussbaum, M., Wright, M.N., Heuvelink, G.B.M., Gräler, B., 2018. Random forest as a generic framework for predictive modeling of spatial and spatio-temporal variables. PeerJ 6, e5518. https://doi.org/10.7717/peerj.5518.

Heung, B., Ho, H.C., Zhang, J., Knudby, A., Bulmer, C.E., Schmidt, M.G., 2016. An overview and comparison of machine-learning techniques for classification purposes in digital soil mapping. Geoderma 265, 62–77. https://doi.org/10.1016/j.geoderma.2015.11.014.

IUSS Working Group WRB, 2015. World reference base for soil resources 2014, update 2015: International soil classification system for naming soils and creating legends for soil maps. World Soil Resources Reports 106.

Jones, M.-F., Arp, P., 2019. Soil Trafficability Forecasting. Open J. Forestry 09 (04), 296–322. https://doi.org/10.4236/ojf.2019.94017.

Keskin, H., Grunwald, S., Harris, W.G., 2019. Digital mapping of soil carbon fractions with machine learning. Geoderma 339, 40–58. https://doi.org/10.1016/j.geoderma.2018.12.037.

Kuhn, M., 2020. *caret: Classification and Regression Training*. Accessed November 09, 2021, https://CRAN.R-project.org/package=caret.

Launiainen, S., Guan, M., Salmivaara, A., Kieloaho, A.-J., 2019. Modeling boreal forest evapotranspiration and water balance at stand and catchment scales: a spatial approach. Hydrol. Earth Syst. Sci. 23 (8), 3457–3480. https://doi.org/10.5194/hess-23-3457-2019.

Li, Z.-L., Leng, P., Zhou, C., Chen, K.-S., Zhou, F.-C., Shang, G.-F., 2021. Soil moisture retrieval from remote sensing measurements: Current knowledge and directions for the future. Earth Sci. Rev. 218, 103673. https://doi.org/10.1016/j.earscirev.2021.103673.

Lidberg, W., Nilsson, M., Ågren, A., 2020. Using machine learning to generate high-resolution wet area maps for planning forest management: A study in a boreal forest landscape. Ambio 49 (2), 475–486. https://doi.org/10.1007/s13280-019-01196-9.

Matthews, B.W., 1975. Comparison of the predicted and observed secondary structure of T4 phage lysozyme. Biochimica et Biophysica Acta (BBA) - Protein Structure 405 (2), 442–451. https://doi.org/10.1016/0005-2795(75)90109-9.

Mattila, U., Tokola, T., 2019. Terrain mobility estimation using TWI and airborne gamma-ray data. J. Environ. Manage. 232, 531–536. https://doi.org/10.1016/j.jenvman.2018.11.081.

McNabb, D.H., Startsev, A.D., Nguyen, H., 2001. Soil wetness and traffic level effects on bulk density and air-filled porosity of compacted boreal forest soils. Soil Sci. Soc. Am. J. 65 (4), 1238–1247. https://doi.org/10.2136/sssaj2001.6541238x.

Meyer, H., Reudenbach, C., Wöllauer, S., Nauss, T., 2019. Importance of spatial predictor variable selection in machine learning applications – moving from data reproduction to spatial prediction. Ecol. Model. 411, 108815. https://doi.org/10.1016/j.ecolmodel.2019.108815.

Mohtashami, S., Eliasson, L., Jansson, G., Sonesson, J., 2017. Influence of soil type, cartographic depth-to-water, road reinforcement and traffic intensity on rut formation in logging operations: a survey study in Sweden. Silva Fennica 51. https://doi.org/10.14214/sf.2018.

Murphy, P.N.C., Ogilvie, J., Arp, P., 2009. Topographic modelling of soil moisture conditions: a comparison and verification of two models. Eur. J. Soil Sci. 60, 94–109. https://doi.org/10.1111/j.1365-2389.2008.01094.x.

Nordfjell, T., Öhman, E., Lindroos, O., Ager, B., 2019. The technical development of forwarders in Sweden between 1962 and 2012 and of sales between 1975 and 2017. Int. J. Forest Eng. 30 (1), 1–13. https://doi.org/10.1080/14942119.2019.1591074.

Nussbaum, M., Spiess, K., Baltensweiler, A., Grob, U., Keller, A., Greiner, L., Schaepman, M.E., Papritz, A., 2018. Evaluation of digital soil mapping approaches with large sets of environmental covariates. SOIL 4 (1), 1–22. https://doi.org/10.5194/soil-4-1-2018.

Oltean, G.S., Comeau, P.G., White, B., 2016. Carbon isotope discrimination by Picea glauca and Populus tremuloides is related to the topographic depth to water index and rainfall. Can. J. For. Res. 46 (10), 1225–1233. https://doi.org/10.1139/cjfr-2015-0491.

Pfeifer, S., Rechid, D., Bathiany, S., 2021. Klimaausblick Deutschland. Accessed November 15, 2021, https://www.gerics.de/imperia/md/content/csc/projekte/klimasignalkarten/gerics_klimaausblick_germany_version1.2_deutsch.pdf.

Picchio, R., Latterini, F., Mederski, P.S., Tocci, D., Venanzi, R., Stefanoni, W., Pari, L., 2020. Applications of GIS-based software to improve the sustainability of a forwarding operation in Central Italy. Sustainability 12 (14), 5716. https://doi.org/10.3390/su12145716.

Poltorak, B.J., Labelle, E.R., Jaeger, D., 2018. Soil displacement during ground-based mechanized forest operations using mixed-wood brush mats. Soil Tillage Res. 179, 96–104. https://doi.org/10.1016/j.still.2018.02.005.

Powers, D.M.W., 2011. Evaluation: from precision, recall and F-measure to ROC, informedness, markedness and correlation. arXiv:2010.1061.

R Core Team, 2020. R: A Language and Environment for Statistical Computing. The R Foundation for Statistical Computing, Vienna, Austria.

Reichle, R., Lannoy, G. de, Koster, R., Crow, W., Kimball, J., Liu, Q., 2020a. SMAP L4 Global 3-hourly 9 km EASE-Grid Surface and Root Zone Soil Moisture Geophysical Data, Version 5. Accessed November 11, 2021, https://nsidc.org/data/SPL4SMGP/versions/3.

Reichle, R., Lannoy, G. de, Koster, R., Crow, W., Kimball, J., Liu, Q., 2020b. SMAP L4 Global 9 km EASE-Grid Surface and Root Zone Soil Moisture Land Model Constants, Version 5. Accessed November 11, 2021, https://nsidc.org/data/SPL4SMLM/versions/5.

Samaniego, L., Kumar, R., Attinger, S., 2010. Multiscale parameter regionalization of a grid-based hydrologic model at the mesoscale. Water Resour. Res. 46, 230. https://doi.org/10.1029/2008WR007327.

Schönauer, M., 2022. R-script to translate SMAP HDF5 files into GeoTIFF format. Zenodo. https://doi.org/10.5281/zenodo.5835820.

Schönauer, M., Maack, J., 2021. R-code for calculating depth-to-water (DTW) maps using GRASS GIS (Version v1). Zenodo. https://doi.org/10.5281/zenodo.5638518.

Schönauer, M., Väätäinen, K., Prinz, R., Lindeman, H., Pszenny, D., Jansen, M., Maack, J., Talbot, B., Astrup, R., Jaeger, D., 2021. Spatio-temporal prediction of soil moisture and soil strength by depth-to-water maps. Int. J. Appl. Earth Obs. Geoinf. 105, 102614. https://doi.org/10.1016/j.jag.2021.102614.

Sørensen, R., Zinko, U., Seibert, J., 2006. On the calculation of the topographic wetness index: evaluation of different methods based on field observations. Hydrol. Earth Syst. Sci. 10, 101–112. https://doi.org/10.5194/hess-10-101-2006.

Southee, F.M., Treitz, P.M., Scott, N.A., 2012. Application of Lidar Terrain Surfaces for Soil Moisture Modeling. *photogramm eng remote sensing* 78 (12), 1241–1251. https://doi.org/10.14358/PERS.78.11.1241.

Vega-Nieva, D.J., Murphy, P.N.C., Castonguay, M., Ogilvie, J., Arp, P.A., 2009. A modular terrain model for daily variations in machine-specific forest soil trafficability. Can. J. Soil Sci. 89 (1), 93–109. https://doi.org/10.4141/CJSS06033.

Venables, W.N., Ripley, B.D., 2002. Modern Applied Statistics with S. Springer, New York.

Wright, M.N., Ziegler, A., 2017. ranger: A fast implementation of random forests for high dimensional data in C++ and R. J. Stat. Soft. 77 https://doi.org/10.18637/jss.v077.i01.

Zeng, L., Hu, S., Xiang, D., Zhang, X., Li, D., Li, L., Zhang, T., 2019. Multilayer soil moisture mapping at a regional scale from multisource data via a machine learning method. Remote Sens. 11 (3), 284. https://doi.org/10.3390/rs11030284.